

Precision beam telescope based on SOI pixel sensor technology for electrons in the energy range of sub-GeV to GeV

Hisanori Suzuki¹, Takumi Omori¹, Kazuhiko Hara¹, Hiroki Yamauchi¹,
Miho Yamada², Toru Tsuboyama³, and Ayaki Takeda⁴

¹*University of Tsukuba, Tsukuba, Ibaraki 305-8571, Japan*

²*Tokyo Metropolitan College of Industrial Technology, Arakawa, Tokyo
116-8523, Japan*

³*High Energy Accelerator Org. (KEK), Tsukuba, Ibaraki 305-0801*

⁴*University of Miyazaki, Miyazaki, Miyazaki 889-2155, Japan*

.....
We developed a beam telescope system comprising five layers of 300- μm -thick INTPIX4NA monolithic pixel sensors. The sensors were fabricated using silicon-on-insulator (SOI) technology. The signal-to-noise ratio of 156–242 was realized at a bias voltage of 20 V. The tracker system was tested using a positron beam of 200–822 MeV/c, and various tracking methods were examined to optimize spatial precision achievable at these energies. The achieved precision results combined with the intrinsic spatial resolution value obtained for a similar system using 120 GeV protons are used to estimate the tracking performance of electrons in the GeV energy range. The estimation method was verified using a GEANT4-based simulation.
.....

Subject Index H12

1 Introduction

Precision beam tracking system is considered essential for detector development especially of such devices targeting an effective spatial resolution. High-energy beams available at CERN and Fermilab are preferred with regard to the multiple scattering of a negligibly small beam; however, accessibility is often limited. In Japan, the Research Center for Electron Photon Science (ELPH), Tohoku University, has demonstrated a positron beam with a maximum momentum of 822 MeV/c [1], and an electron beam of 1–5 GeV/c at AR-TB has been commissioned at the High Energy Accelerator Research Organization (KEK) [2]. We have initiated a research and development to develop a precision beam telescope system that can be operated at the aforementioned energy values.

Silicon-on-insulator (SOI) semiconductor technology has been adopted for monolithic pixel sensor fabrication, and an integration-type sensor, INTPIX4 [3][4], is one of the large sensors (sensitive area is $14.1 \times 8.7 \text{ mm}^2$), with each pixel size of $17 \mu\text{m}$ square, fabricated using the 0.2- μm fully-depleted SOI technology of Lapis Semiconductor.

The telescope comprises five layers of $300 \mu\text{m}$ thick INTPIX4NA, the revised version of INTPIX4, with another beam-triggering SOI pixel sensor, XRPIX5 [5], located at the rear of the system. INTPIX4NA and XRPIX5 are equipped with a function defining the region of interest (RoI). The telescope system was tested at ELPH for the positron beam at 200–822 MeV/c. As one of the five sensors has been set as a device under test (DUT), the DUT hit position and the intercept of the track reconstructed by other systems are compared to evaluate the performance of the telescope. The track reconstruction was examined considering various combinations of the tracking layers. Moreover, the tracking performance was evaluated when a 2 mm-thick-aluminum plate was inserted to simulate the performance for a thicker DUT.

The tracking residuals obtained for the beam momentum of 200–822 MeV/c combined with the previous data obtained using protons of 120 GeV [6] were used to estimate the tracking performance in the defined GeV range at the KEK AR-TB. A simulation based on GEANT4 was also conducted to examine the estimated results.

2 The beam telescope with regard to the ELPH beamline

2.1 INTPIX4NA sensor and SEABAS2 readout system

The integration-type pixel sensor, INTPIX, is one of the SOI sensors that are been actively developed. The main parameters of INTPIX4 are listed in Table 1 [3]. The thicknesses of INTPIX4 and INTPIX4NA are 500 and $300 \mu\text{m}$, respectively.

Table 1 Main parameters of the INTPIX4 sensor.

Chip size	$15.4 \times 10.2 \text{ mm}^2$
Active area	$14.1 \times 8.7 \text{ mm}^2$
Pixel size	$17 \times 17 \text{ }\mu\text{m}^2$
Pixel array	512 (row) \times 832 (col) 13 blocks (64 cols) for parallel readout
Wafer	n-FZ, $\sim 11 \text{ k}\Omega\text{cm}$ (INTPIX4NA)

INTPIX4 employs a correlated differential sampling method to suppress the noise associated at switching. The charge integrated for predetermined duration ($9 \text{ }\mu\text{s}$ at ELPH testbeam) is reset periodically unless the STORE signal is received. The STORE triggers readout sequence, holding the charges stored in the capacitors and sending them one-by-one to external 12-bit analog-to-digital converters (ADCs). The groups of 64-column data (times 512 row data) are fed into one ADC, overall, 13 ADCs are operating simultaneously. The digitization time per pixel, including switching time to the next pixel data, (or pixel scan time), was set to 200 ns at the testbeam, whereas it functions reliably at a scan time of 150 ns.

The readout of each INTPIX4NA sensor is controlled by the SEABAS2 [4] readout system. SEABAS2 is equipped with two field-programmable data arrays (FPGAs), one (Virtex-5) for user programming and another (Virtex-4) for data transfer with 1 GbE SiTCP protocol. The ADCs and digital-to-analog converters are located on the SEABAS2 board.

The INTPIX4NA chip is glued to a separate board, i.e., a sub-board, which is connected to the SEABAS2 board via a pair of 64-pin connectors. The complete structure is shown in Figure 1.

2.2 The telescope with regard to the ELPH positron beam

The telescope system comprises five INTPIX4NA sensors and one XRPIX5 sensor at the downmost-stream position. They are interleaved at an equi-distance of 32 mm (Figure 2). The SEABAS2 board is screwed to a 2-mm thick aluminum board whose height is 20 cm and width is 40 cm. Six aluminum boards are subsequently screwed using 30-mm long spacers. The sub-boards of the five sensors are aligned using three precision threading stainless rods (Figure 1) at a precision of $5 \text{ }\mu\text{m}$.

The data acquisition sequence is controlled by USAGI with an FPGA. USAGI distributes synchronized RESET signals at a 100 kHz frequency and 1 kHz timestamp signals to the five INTPIX4NA chips. On receiving the beam trigger signal from XRPIX5, USAGI disables

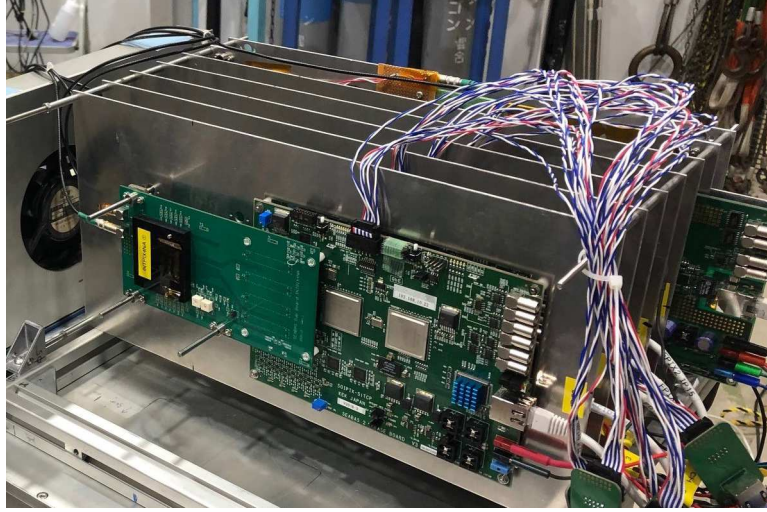


Fig. 1 The telescope system placed in the ELPH beam, viewed from beam upstream. There are five INTPIX4NA sensors, followed by one XRPIX5 sensor. The sensor is located behind the black block (the beam window at center is taped in this photo) on the sub-board, which is connected to the SEABAS2 board. The control signals (RESET, STORE, TimeStamp Clock, BUSY) are transmitted through the 10-pin connector at the top of SEABAS2 board, with the ADC data extracted through the RJ-45 connector at right. The supporting aluminum boards are 20 cm high and 40 cm wide.

XRPIX5 to generate further triggers and sends the STORE signal. Then, the INTPIX4NAs terminate generating further RESET signals and the readout sequence is initiated individually in each SEABAS2 board. The timestamp count is attached to the data to verify the simultaneity of the hits. The inactive INTPIX4NA while being periodically reset are not exactly synchronized among the five layers; however more than 99% of the data have been found to be synchronized. The USAGI receives BUSY signals from the SEABAS2 boards and clears the XRPIX5 disable signal once all the BUSY signals are cleared.

The telescope system possesses a beam window, and only sensors with a thickness of $300\ \mu\text{m}$ are exposed to the beam. Later, we placed a 2-mm thick aluminum plate before L4, as illustrated in Figure 2, to mimic additional materials and investigate the effect of the materials, or thicker DUT, on beam tracking.

The ELPH provided positron beams with a maximum momentum of $822\ \text{MeV}/c$. The photons of the ELPH 1.3 GeV electron synchrotron are converted on a $200\text{-}\mu\text{m}$ thick tungsten target, and the positrons with specific momentum are selected with a relative spread of 0.85% for a beam of $822\ \text{MeV}/c$. Most measurements were performed at this momentum. Moreover, low momenta, down to $200\ \text{MeV}/c$, were considered to examine the momentum dependence.

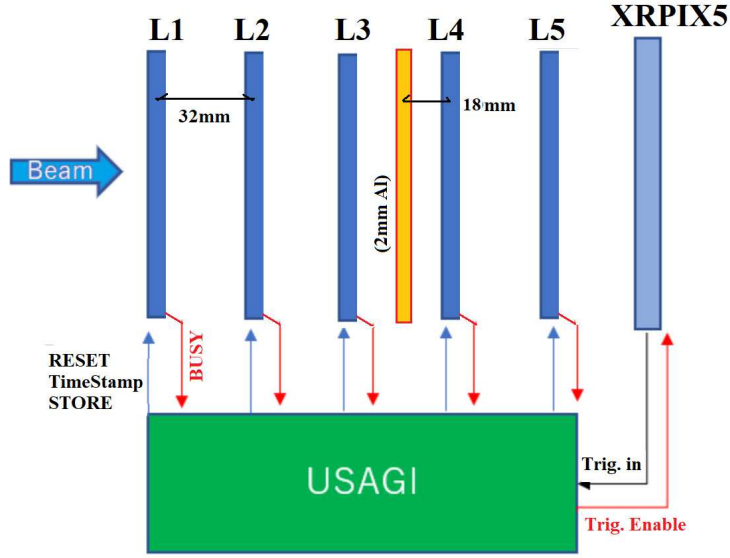


Fig. 2 Five telescope layers followed by one XRPIX5 sensor, with the trigger logic unit (USAGI). A 2-mm thick aluminum plate, shown in orange, was placed later in the measurement to mimic the effect of additional material.

The relative momentum spreads are 2.5% at 200 MeV/c, 1.8% at 300 MeV/c, and 1.2% at 500 MeV/c [7].

The positron beam was extracted for ~ 10 s followed by a quiet time of 7 s. The beam was transmitted through a set of quadrupole magnets with the resulting beam profile at the telescope being wide enough, such that the beam distributions were almost flat along the horizontal and vertical directions.

3 Performance evaluation using the ELPH positron beam

3.1 Cluster charge (CC) and signal-to-noise (S/N) ratio

The pedestal of individual pixel is calculated by averaging the ADC values obtained based on the beam data. Simple averages resulted in the pedestal rms spreads σ_{ped} of 4–8 ADCs fluctuating among the data taking runs. The main reason is the abrupt fluctuations across all the pixels with an almost constant amount. Pedestal corrections based on a frame considering 1 common value or 13 values per readout block reduce the pedestal fluctuation, resulting in σ_{ped} of 1.9–2.8 ADCs with a single value or 1.6–2.2 ADCs with 13 value corrections. We adopted the pedestals with per block frame correction (13 value corrections) in the following analysis.

Clustering is a step to correlate the pixel data to the beam hit. We define a cluster of the pixels with more than 10σ of pedestal (typically more than 20 ADC counts) about the seed pixel possessing the largest signal. Figure 3 shows the distribution of cluster sizes (CS) defined by the number of pixels included in a cluster, and CCs of the L3 sensor operated at 20 V bias. The cluster size distribution has a mean of 7.8 pixels extending up to 20 pixels. The CS exhibits a Landau distribution (overlaid in the plot) with a most probable value (MPV) of 381 ADCs.

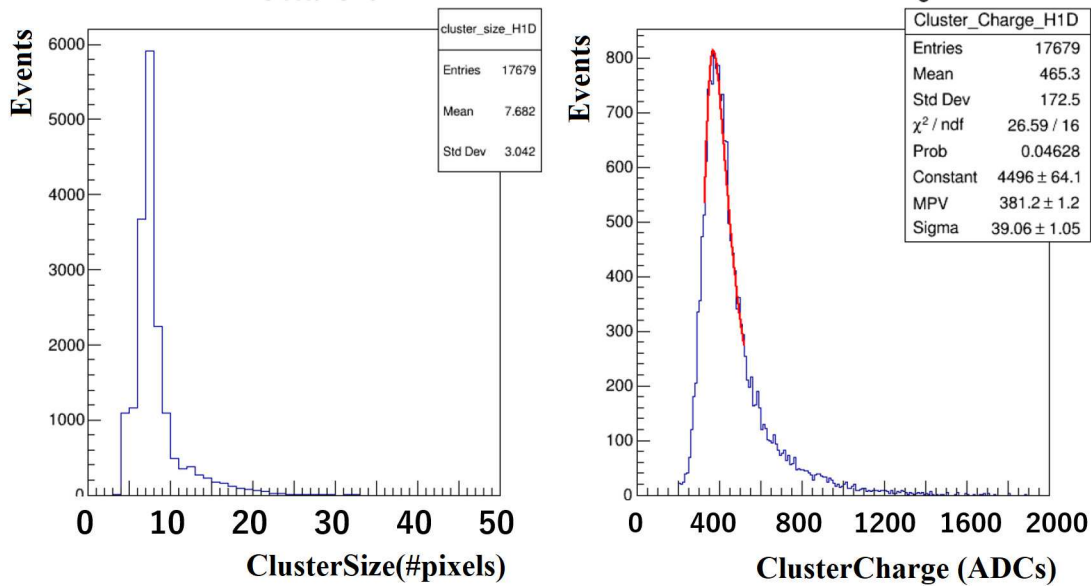


Fig. 3 The distribution of number of pixels in a cluster (left) and of the cluster charge (right) of L1 INTPIX4NA sensor at 20 V bias voltage.

The MPVs of CC distributions and pedestal sigmas (σ_{ped}) obtained at 20 V are listed in Table 2, along with the S/N ratios.

3.2 HV dependence of cluster characteristics

The bias voltage dependence of the CCs is plotted in Figure 4. The curve exhibits a plateau ~ 30 V, implying that the sensor is fully depleted. The full depletion voltage defined by the voltage of the intercept where the plateau constant and linear line fitted to CC vs. V_{bias} data points ranged from 26 (L1 and L5) up to 38 V (L4). As the nominal wafer resistivity is in the range of 10.1–12.1 $\text{k}\Omega\text{cm}$, the expected full depletion voltage is in the range of 27–33 V for 300- μm -thick n -type silicon; the estimation is almost consistent with the measured voltages.

Table 2 S/N ratios at 20 V bias for the five layers. Noise and signal values are defined in the unit of ADCs.

layer	noise	signal	S/N
L1	1.6	381	237
L2	1.8	339	188
L3	1.8	354	188
L4	1.7	275	156
L5	1.6	383	242

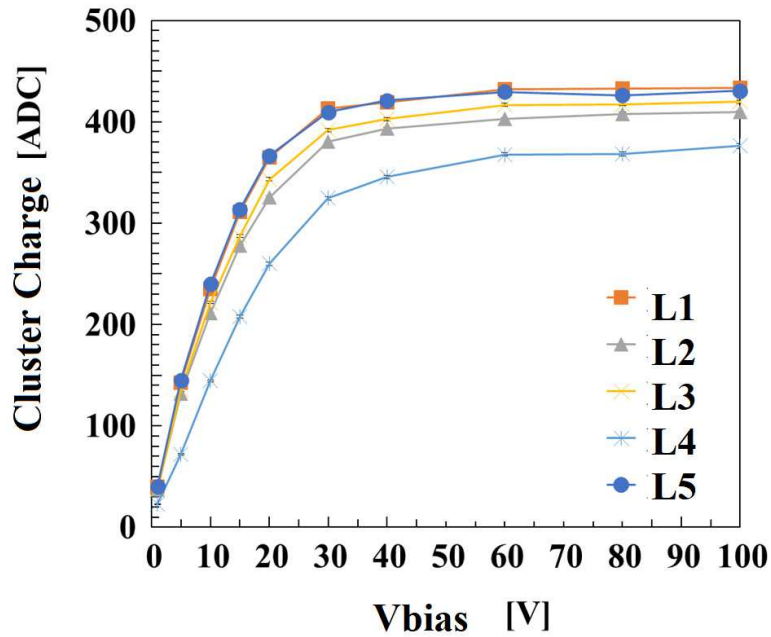


Fig. 4 The most probable CC values as a function of bias voltage shown for five INTPIX4NA sensors.

The bias voltage dependence of the CSs is plotted in Figure 5. As an adequate charge spread with regard to the hit position sharing the charge among multiple pixels is a key for effective spatial resolution, the curves are characterized; the CS increases with the bias below the full depletion level as the carrier drift length increases and decreases above the level as the electric field increases; diffusion effect is suppressed.

We observe slight variations in the S/N, CC, and CS distributions among the five layers. This is explained by the individual variation in INTPIX4NA gain settings [3] in the SEABAS2 boards. However, the bias dependence curves are uniform among the five layers.

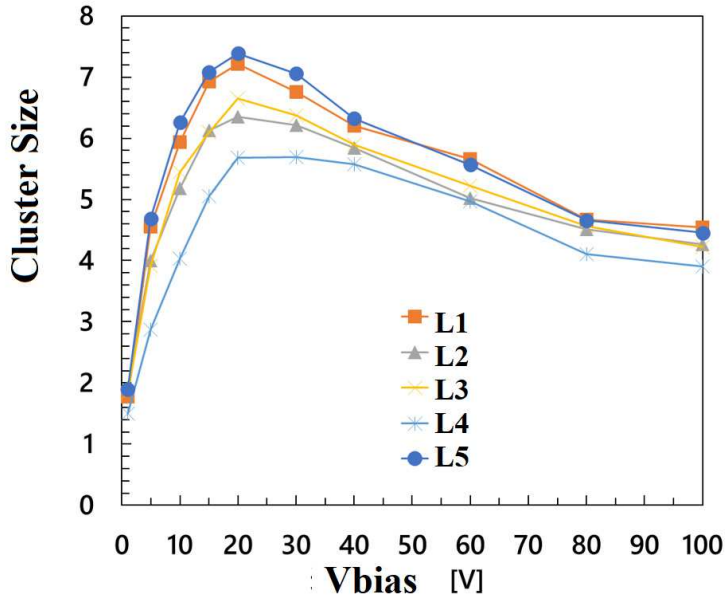


Fig. 5 The mean number of pixels in a cluster (cluster size) as a function of bias voltage shown for five INTPIX4NA sensors.

3.3 Tracking precision for 822 MeV/c positrons

The hit position is defined by the ADC-averaged weight mean of the hit pixels' positions. Tracks are defined by the hits of a certain combination of layers excluding the detector layer under test (DUT). The tracking precision is defined as the standard deviation of the hit residuals of DUT with respect to the track intercepts. The tracking precision study was performed by changing the DUT and combinations of tracking layers.

In high-energy hadron beams available at CERN and Fermilab, the detector intrinsic spatial resolution is obtained by fitting the detector hits to a straight line as the effects of multiple scattering is negligibly small. The intrinsic resolution of the INTPIX4 derived is 1.34–1.65 μm [6], as described in Section 4.1.

For the electrons with 822 MeV/c, the tracking has to be optimized considering the multiple scattering. As listed in Table 3, first, we consider a tracking using a tracing method (a) one layer in each side of the DUT. Secondly, two layers are on one side and one layer is on the other side of the DUT. In this case, three layer hits are fitted to a straight line. The intercept at the DUT is calculated (b) using the fitted track or (c) using the hit located just in front of the DUT and the track slope in the case of two layers in front, and similarly (d) or (e) using the hit located just rear of DUT and the track slope for the case of two layers on the rear side. The results are listed in Table 3. The values vary slightly base on the

Table 3 Residual sigmas [μm] for 822-MeV/c positrons measured at 20 V bias. Two values in each field are measured along the X and Y directions. See text for explanation of tracking method. (j) uses the average of the intercepts obtained using methods (c) and (e).

Tracking method	DUT			Average
	L2	L3	L4	
(a) 1-1	12.06 \pm 0.10/11.91 \pm 0.10	12.15 \pm 0.10/12.24 \pm 0.10	12.71 \pm 0.12/12.98 \pm 0.11	12.34 \pm 0.11
(b) 2-1	-	14.42 \pm 0.12/14.54 \pm 0.12	14.91 \pm 0.13/15.33 \pm 0.13	14.80 \pm 0.12
(c) 2*-1	-	11.80 \pm 0.10/11.72 \pm 0.12	12.23 \pm 0.10/12.40 \pm 0.10	12.04 \pm 0.11
(d) 1-2	14.32 \pm 0.12/14.27 \pm 0.17	14.48 \pm 0.12/14.48 \pm 0.12	-	14.39 \pm 0.12
(e) 1-*2	11.72 \pm 0.10/11.63 \pm 0.10	12.18 \pm 0.10/12.22 \pm 0.12	-	11.94 \pm 0.11
(f) 2-2	-	20.28 \pm 0.16/20.54 \pm 0.17	-	20.31 \pm 0.17
(g) 2*-2	-	14.57 \pm 0.12/14.63 \pm 0.17	-	14.60 \pm 0.15
(h) 3-1	-	-	16.28 \pm 0.14/16.11 \pm 0.14	16.20 \pm 0.14
(h) 3*-1	-	-	15.27 \pm 0.12/14.27 \pm 0.17	14.77 \pm 0.15
(h) 1-3	14.32 \pm 0.12/14.27 \pm 0.17	-	-	14.30 \pm 0.15
(i) 1-*3	14.87 \pm 0.14/15.02 \pm 0.12	-	-	14.95 \pm 0.13
(j) <(c),(e)>	-	11.10 \pm 0.10/10.98 \pm 0.09	-	11.04 \pm 0.10

selection of the DUT and horizontal/vertical directions, which should be explained by the differences on the individual detector and mostly by the residual miss-alignments. Averages of the values are also shown in the table.

Method (a) provides an optimal value of 12.34 \pm 0.11 μm , and any additional hit information degrades the tracking precision, unless the hit nearest to the DUT is used as anchor (c) or (e), where slightly better residual of 12 μm has been obtained. The best performance 11 μm is obtained for method (j) where the tracker positions obtained using methods (c) and (e) are averaged. The intrinsic INTPIX4 resolution is included in these values; however, the value of \sim 1.5 μm is considerably smaller and not subtracted.

The bias dependence of (c) 2*-1 tracking precision with L3 chosen as the DUT is plotted in Figure 6. The dependence is weak, where the spatial resolution improves with a decrease in the bias except at 2 V. At 2 V, the S/N ratio is roughly 1/10 of that at 20 V, and the charge spread is not large enough.

As a good spatial resolution is realized by adequate charge spread among pixels with good S/N, the use of the SOI sensor that can realize fine pixel size and superior S/N is the key for the high-performance tracker. For example in [8], we demonstrated that the intrinsic position resolution of SOI pixel sensor FPIX with 8- μm pixel size and S/N of \sim 300 is 0.60–0.75 μm , the first semiconductor device with sub-micron spatial resolution.

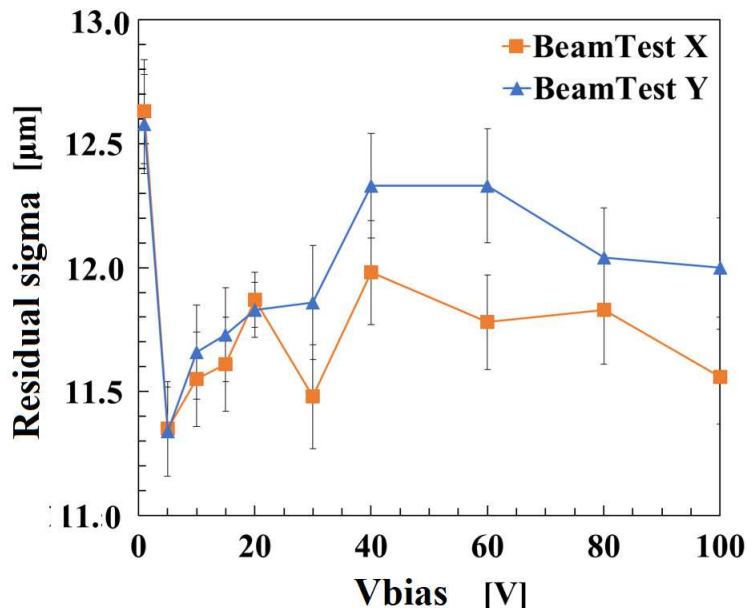


Fig. 6 The residual sigma of 2*-1 tracks with respect to L3 hits as a function of bias voltage, demonstrated in X and Y directions.

3.4 Tracking with additional material

Tracking may need to be optimized for different thickness of the DUT. In the ELPH beam line, we added a 2-mm-thick aluminum plate between L3 and L4 (Figure 2). One of the most robust tracking methods against material is to use two tracks reconstructed using the layers in front and those at rear. Figure 7 plots the distribution of the position along the beam defined as the intersection of the track given by L1 and L2, and that given by L4 and L5. The mean value of 78.7 mm with regard to L1 is consistent considering the location of the aluminum plate. The position calculated as the average of the extrapolation points of the two tracks is denoted as method (k).

Table 4 lists the effect of 2-mm-thick aluminum plate on the tracking residual sigmas for a few tracking methods. Method (c) 2*-1 is significantly affected by the additional material, whereas method (j) maintains the best performance for both cases. Method (k) also exhibits negligible degradation though the value is larger than the other methods.

In the case of very thick DUT, like a calorimeter, we need to use the track reconstructed using the layers in front only. We obtain $24.46 \pm 0.21 \mu\text{m}$ for 2-0 (0 means that no layer at rear is used) and $27.82 \pm 0.23 \mu\text{m}$ for 3*-0. We observe that the third layer does not improve the resolution as multiple scattering is significant. The 3*-0 track performance improves and becomes comparable with the 2-0 track performance by selecting small χ^2 3*-0 tracks. We

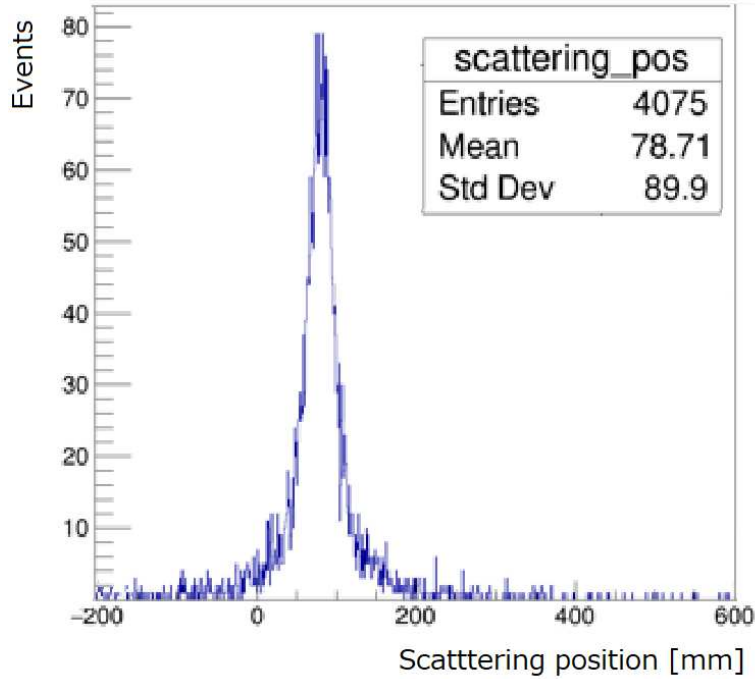


Fig. 7 The scattering position in Z given by the closest approach point of L1–L2 and L4–L5 tracks.

Table 4 Residual sigmas [μm] for 822 MeV/ c positrons measured at 20 V bias. The values are for DUT = L3 compared with and without the 2-mm-thick aluminum. Tracking methods (c) and (j) are same as in Table 3. (k) refers to the average position of the tracks reconstructed separately in front and at the rear of the DUT.

tracking method	without Al	with Al
(c) 2*-1	11.78 \pm 0.12	15.27 \pm 0.21
(j) <(c),(e)>	11.04 \pm 0.10	11.60 \pm 0.19
(k) <2,2>	17.55 \pm 0.17	18.76 \pm 0.26

propose to locate three layers in front of the thick DUT and use 2-0 tracks provided that $3^*-0 \chi^2$ is reasonably small, which reject spurious tracks created artificially such as by noise in the 2-0 tracks.

4 Tracking precision expectation for electrons within the GeV energy range

4.1 Intrinsic resolution evaluation with 120-GeV protons

We evaluated the intrinsic INTPIX4 resolution [6] using 120-GeV protons at the Fermilab Test Beam Facility in 2018. The tracker system is similar to the current system except that the three DUTs set at the middle were other SOI sensors, SOFIST [10], being developed for the ILC experiment, and the thickness of tracker INTPIX4 sensors was $500 \mu\text{m}$ instead of $300 \mu\text{m}$ of INTPIX4NA. The sensor thickness difference can be ignored as multiple scattering is negligible and CS distributions were very similar to those obtained at the ELPH beam test; the mean values ranged from 7.2 to 9.3 for the four INTPIX4 trackers.

At the equidistant spacing of 32 mm, three SOFIST sensors were set at the middle with the four INTPIX4 sensors set as L1, L2, L6 and L7. Figure 8 shows the residual of the sensor hits to the tracks reconstructed using the other three INTPIX4 sensors. The Gaussian sigmas ranged from 1.77 to $2.55 \mu\text{m}$. After subtracting the tracker resolution, the intrinsic resolution ranged from $1.34 \pm 0.05 \mu\text{m}$ (for L2) to $1.65 \pm 0.09 \mu\text{m}$ (for L7). The average value of the obtained intrinsic resolutions $1.50 \pm 0.15 \mu\text{m}$ is considered as the intrinsic spatial resolution of INTPIX4NA where the uncertainty is the maximum deviation of the four estimated values.

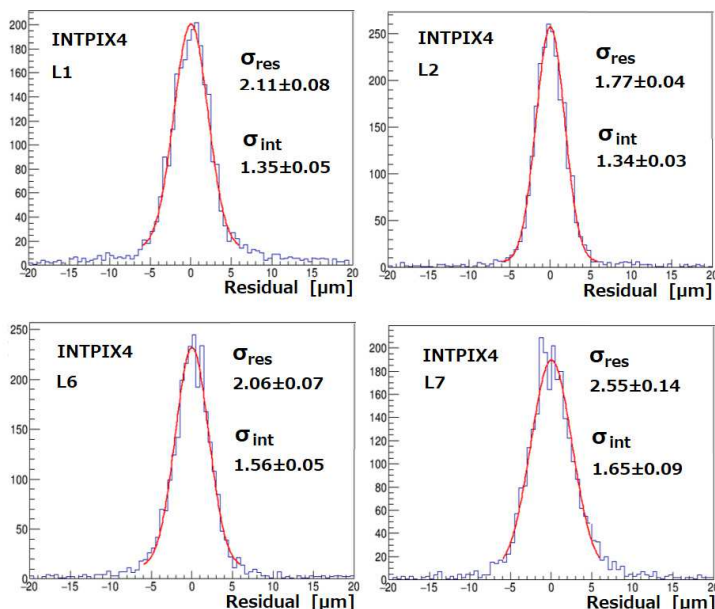


Fig. 8 The tracker residual distributions of four INTPIX4 sensors measured using 120-GeV protons. σ_{res} is of the fitted Gaussian, and σ_{int} is the intrinsic sensor resolution corrected for the tracker uncertainty. The unit is in μm .

4.2 Estimation of tracking precision in GeV energy range

The intrinsic resolution of $1.50 \pm 0.15 \mu\text{m}$ corresponds to the 2-1 track residual sigma of $1.84 \pm 0.18 \mu\text{m}$ at 120 GeV, where the uncertainty originates from the uncertainty of INTPIX4 intrinsic resolution described above. The obtained value and four 2*-1 residual sigmas measured at the four momenta at ELPH are fitted to the following function;

$$\sigma_{\text{res}}(p) = \sqrt{\sigma_0^2 + (k/p)^2}, \quad (1)$$

with resulting values of $\sigma_0 = 1.84 \pm 0.18 \mu\text{m}$ and $k = 9.023 \pm 0.077 \mu\text{m}\cdot\text{GeV}/c$. The data points and fitted function are plotted in Figure 9.

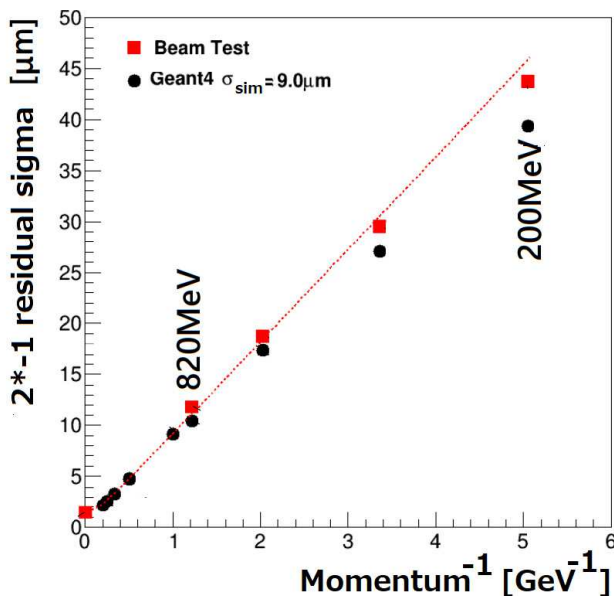


Fig. 9 The residual sigma of 2*-1 tracks with respect to the L3 hits as a function of 1/momentum.

Also plotted in the figure are the evaluations at ELPH momentua and 1-5 GeV electrons based on a GEANT4 [9] simulation. While GEANT4 precisely traces the electron trajectory considering detailed physical interactions with the material, the conversion from the energy deposition in the sensor to the pixel charge spread needs to be implemented additionally. Instead of relying on dedicated simulation such as TCAD, the beam data were used to parameterize the charge spread.

The distribution of pixel charges normalized by the maximum pixel charge in an event was projected in horizontal or vertical direction, and then, the projected distribution was fitted with a Gaussian function. Figure 10 shows the Gaussian sigmas σ_{spread} on the ordinate axis

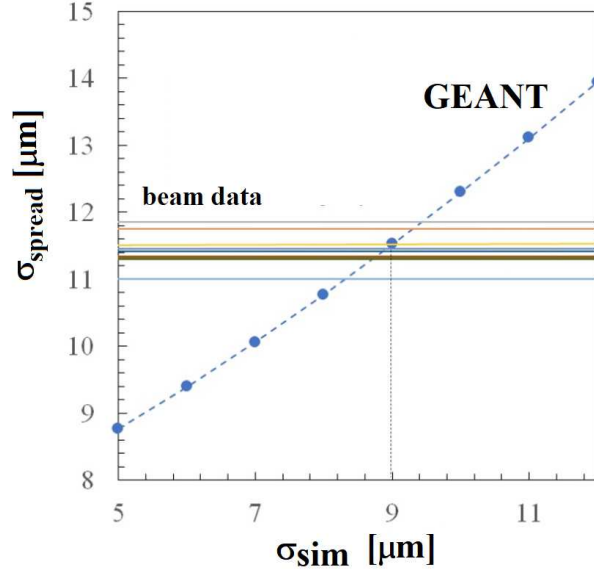


Fig. 10 The relation between the Gaussian charge spread σ_{sim} implemented in the simulation and the pixel charge spread σ_{spread} about the seed pixel. σ_{spread} values obtained in the beam data for five layers and X and Y directions are shown in the ordinate axis.

obtained in the ELPH beam for the five layers in X and Y directions. The value ranges from 11.0 to $11.8 \mu\text{m}$. In the Geant4 simulation, the deposited energy was distributed according to Gaussain with a given spread σ_{sim} in the X and Y directions, and the pixel charges were defined as the integral of the charge in the corresponding pixel area of $17 \times 17 \mu\text{m}^2$. The electron beam was injected uniformly across the pixel surface. With an increase in the σ_{sim} value, σ_{spread} obtained with regard to the beam data increases as shown in the figure. The optimum σ_{sim} was set to $9 \mu\text{m}$ from this plot. Further steps were added in the simulation to correct for the charge spread in the pixels apart from the seed pixel and for the finite ADC pedestal spread.

The 2^*-1 track residual sigma estimated for 5-GeV electrons is $2.68 \pm 0.14 \mu\text{m}$ (Equation (1)) and $2.21 \pm 0.02 \mu\text{m}$ based on the Geant4 simulation. The difference in the estimation should originate in (I), where the beam data overestimate the resolution as there is residual layer misalignment, and (II), where the simulation does not consider for event-by-event fluctuation in the charge spread nor position dependence in the pixel surface, generating an underestimated value.

5 Comparison with the existing tracker and possible system improvements

5.1 Comparison with the EUDET tracker

One of the performance beam trackers suitable for electron energy ranging from sub-GeV to GeV is EUDET beam telescope [11] based on MIMOSA26 monolithic active pixel devices. The MIMOSA26 sensor consists of pixels sized $18.4 \times 18.4 \mu\text{m}$ and a sensor thickness of $54 \mu\text{m}$. For 6 GeV electron/positron beam, the spread of the biased residual distribution, including tracker and DUT resolutions, was $2.88 \pm 0.08 \mu\text{m}$. By subtracting the DUT intrinsic resolution of $3.24 \pm 0.09 \mu\text{m}$, the track resolution using an equidistant plane spacing of 20 mm is estimated to be $1.83 \pm 0.03 \mu$ for 5-GeV electrons.

By subtracting the INTPIX4NA intrinsic resolution of $1.5 \mu\text{m}$, the values mentioned in the previous section correspond to $2.22 \mu\text{m}$ of the beam data and $1.62 \mu\text{m}$ of the Geant4-based simulation; the values are comparable to the EUDET evaluation.

5.2 DAQ rate and possible improvement

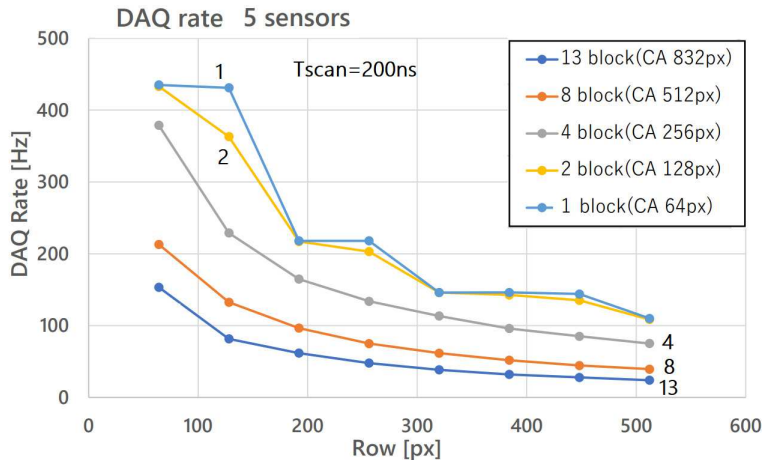


Fig. 11 The DAQ rate of the 5-layer system as a function of the number of readout row pixels and for the number of readout column blocks (each block contains 64 columns). The pixel scan scan time is set to 200 ns.

The present tracker system employs a switching hub to collect all the five layers of INTPIX4NA data and one layer of the XRPIX5 data to a computer. The DAQ rate when all the five layers are read out is plotted in Figure 11 as a function of the number of readout row pixels (up to 512) for various settings of the number of readout column blocks (up to 13). The DAQ rate of single sensor is primarily determined based on the pixel scan time,

which is 200 ns in this data sample. As the system can be operated at 150 ns, the rate will increase accordingly. The scan time as a 5-layer system is degraded further with an increase in the number of readout blocks, thereby implying that the data transfer rate to the computer limits the overall rate. By reducing the amount of transfer data by employing zero-suppression in the FPGA, the rate should recover to 105 Hz. The curves of 1-block and 2-block readout schema are almost identical; therefore, the DAQ rate is not limited by the data transfer up to 2-block readout.

As described before, the analog signals generated from INTPIX4NA are digitized using 12-bit ADCs located in the SEABAS2 board. By placing ADCs near to the INPIX4NA chip on the sub-board should help reduce the scan time. The simulation suggests that a scan time of 100 ns should be possible. Ultimate improvement is implementation of column ADCs as successfully implemented in SOFIST [10].

5.3 Improvement with thinner sensors

The bias voltage dependence of residual sigma shown in Figure 6 ensures that the tracking performance does not degrade much at a bias of 5 V, where the average CC is 140 ADCs (40% of the cluster charge at 20 V). To improve the tracking performance of low-energy electrons using thinner sensors, we have estimated the performance when the sensors are 60 μm or 130 μm thick using the same GEANT4-based simulation with the same setting of $\sigma_{\text{sim}} = 9 \mu\text{m}$. The simulation results are illustrated in Figure 12, where 2*-1 track residual sigma values are plotted as a function of electron momentum. In this range, the tracker system with 130- μm thick sensors exhibits the best performance, whereas the system with 300- μm sensors degrades more at lower momenta as expected. The performance of 60- μm thick sensors does not improve with momentum as the signal size is small, thereby generating low S/N. The constructed system using 300- μm thick sensors similarly performs for 5-GeV/c electrons.

6 Summary

We have constructed a beam tracker using INTPIX4NA SOI pixel sensors and evaluated the tracking performance of electrons within sub-GeV energy range. Various tracking methods were examined, and the best residual sigma of $11.04 \pm 0.10 \mu\text{m}$ was obtained for 822-MeV/c electrons, including the DUT intrinsic resolution of $1.50 \pm 0.15 \mu\text{m}$. The performance tracking method obtained for 300- μm DUT thickness did not degrade when also for the case when the 2-mm aluminum plate was added.

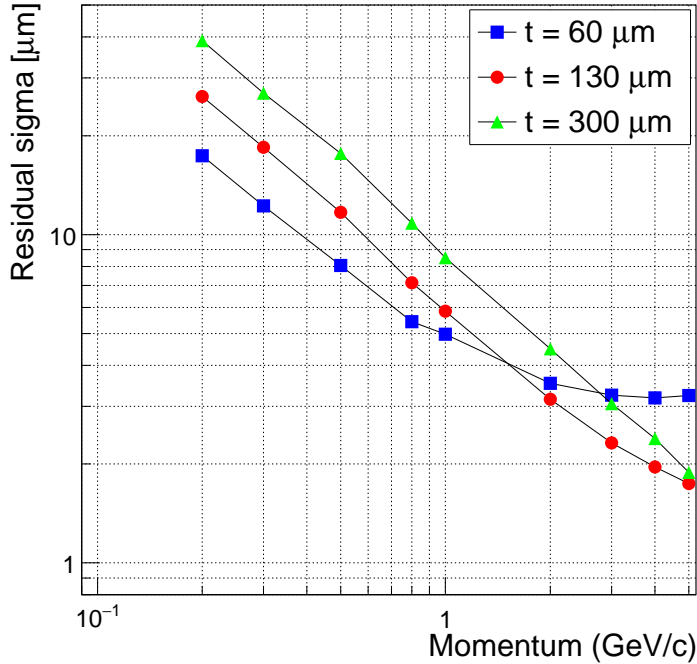


Fig. 12 2^*-1 track residual sigmas as a function of electron momentum estimated using Geant4 based simulation for the sensor thicknesses of 60, 130 and 300 μm .

The measured data combined with the data derived using 120-GeV protons were used to evaluate the performance of GeV electrons. The Geant4-based simulation describes the measured results reasonable well. The tracker resolutions, including the intrinsic DUT resolution, were estimated to be 2.68 μm of the beam data and 2.21 μm of the Geant4-based simulation for 5 GeV electrons.

Acknowledgments

We would like to thank personnel of the ELPH accelerator, Tohoku University, and the Fermilab Test Beam Facility for providing beams in excellent condition throughout the experiment. Expert advice and suggestions provided by Prof. Yasuo Arai and Dr. Toshinobu Miyoshi, designers of INTPIX4, and by Dr. Ryutaro Nishimura, DAQ system developer, were valuable for conducting this study. We also thank Mr. Kyoya Misumi of Miyazaki University for helping in data acquisition at the ELPH. The current study was supported by the Tomonaga Center for the History of the Universe (TCHoU) of University of Tsukuba and KAKENHI (19H00692).

References

- [1] ELPH homepage: <https://www.lns.tohoku.ac.jp/en/>
- [2] K. Hanagaki, High Energy News, **39-2** (2020) (in Japanese).
- [3] Y. Arai, “INTPIX4 User’s Manual”, <https://soipix.jp/content/documents/INTPIX4doc.v032.pdf>
- [4] R. Nishimura et al., “DAQ Development for Silicon-On-Insulator Pixel Detectors”, Proc. of Int. Workshop on SOI Pixel Detector (SOIPIX2015), June 3-6, 2015, Sendai, Japan; arXiv:1507.04946v1.
- [5] H. Hayashi et al., Nucl. Instr. Methods A924, 400–403 (2019)..
- [6] H. Yamauchi, “Performance of a tracking system constructed using large area INTPIX4 SOI pixel detectors evaluated in 120 GeV beam (in Japanese)”, Master thesis, University of Tsukuba (2019).
- [7] T. Ishikawa, “Electron · positron beamline V (in Japanese)”, HD no. 440E, Nov 2020.
- [8] K. Hara et al., “Development of Silicon-on-Insulatpr Devices”, PoS(Vertex2017) 035, 2018.
- [9] J. Allison et al., “Geant4 developments and applications”, IEEE TNS 53-1, 270–278 (2006).
- [10] H. Murayama et al., Nucl. Instr. Methods A978, 164417 (2020).
- [11] H. Jansen et al., arXiv:1603.09669v2 [physics.ins-det] (2016).